S. M. Riaz, M. C. Lucas-Estañ, B. Coll-Perales and J. Gozalvez, "Predictive Configured Grant Scheduling for Deterministic Wireless Communications", *Proc. of the 2025 IEEE 101st Vehicular Technology Conference (VTC2025-Spring)*, Oslo, Norway, 2025, pp. 1-5. DOI: 10.1109/VTC2025-Spring65109.2025.11174458.

Predictive Configured Grant Scheduling for Deterministic Wireless Communications

Syed Morsleen Riaz, M.Carmen Lucas-Estañ, Baldomero Coll-Perales, Javier Gozalvez
Uwicore laboratory, Universidad Miguel Hernández de Elche, Elche (Alicante), Spain
sriaz@umh.es, m.lucas@umh.es, bcoll@umh.es, j.gozalvez@umh.es

***Abstract*— Future wireless networks must enhance their capacity to sustain deterministic service levels and support emerging time-sensitive services in key verticals. The ability to guarantee bounded latencies heavily depends on efficient radio resource management. Configured Grant (CG) scheduling can reduce latency by pre-allocating resources, but its effectiveness and efficiency decrease under variable traffic patterns. This study presents a novel predictive CG scheduling scheme that pre-allocates resources based on traffic predictions while accounting for prediction inaccuracies. By considering these inaccuracies, the scheme significantly improves the ability to meet bounded latency requirements, which are essential for supporting deterministic service levels. Our evaluations show that the proposed scheme significantly enhances the capacity to support deterministic service levels while improving resource utilization, even in scenarios with variable and mixed traffic flows with diverse requirements.**

Keywords—scheduling, configured grant, predictive, deterministic, time-sensitive, 5G, 6G.

I. Introduction

5G networks were designed to support ultra-reliable low-latency communications (URLLC) and new verticals such as smart mobility and manufacturing. However, the increasing digitalization and automation in these verticals introduce new challenges to support deterministic services with stringent bounded latency requirements. To meet these demands, future networks must support deterministic communications while accommodating mixed traffic flows with varying characteristics and diverse QoS (Quality of Service) requirements. The ability to sustain deterministic service levels relies heavily on efficient and effective radio resource management, including advanced scheduling mechanisms that can anticipate demands and dynamically schedule transmissions in mixed traffic environments.

5G and beyond can reduce latencies through semi-static scheduling schemes, which include Configured Grant (CG) for uplink (UL) transmissions and Semi-Persistent Scheduling (SPS) for downlink (DL) transmissions. Semi-static scheduling eliminates the need to send a Scheduling Request (SR) and/or wait for a Scheduling Grant before transmitting a data packet, instead pre-allocating resources to nodes so they can immediately transmit packets upon generation. Semi-static scheduling has proven highly effective in ensuring low transmission latencies for periodic traffic with fixed packet sizes. However, its effectiveness and efficiency decrease in scenarios where packet sizes vary, message periodicity fluctuates or does not align with the periodicity of resource allocation [1], or when multiple traffic flows with different periodicities coexist [2]. To address these inefficiencies, current approaches explore predictive scheduling mechanisms that anticipate traffic demands. Studies such as [3] propose semi-static scheduling schemes that pre-allocate or reserve resources based on traffic predictions. However, such pre-allocations are prone to inefficiencies due to prediction inaccuracies and the inherent stochasticity of wireless systems. These inefficiencies can negatively impact overall system capacity and compromise the ability to guarantee bounded latency requirements for deterministic services [3]. In this context, this work proposes a novel predictive Configured Grant (CG) scheduling scheme that accounts for inaccuracies in traffic predictions when pre-allocating radio resources based on anticipated traffic demands. The proposed CG scheduling scheme is designed to support deterministic service levels in scenarios with mixed traffic flows and diverse QoS requirements. Rather than minimizing transmission latency, the scheme aims to maximize the percentage of transmissions that meet their bounded latency requirements. By leveraging predicted traffic information along with potential prediction inaccuracies, the scheme pre-allocates resources with a high likelihood of meeting bounded latency requirements. Our evaluation demonstrates that the proposed predictive CG scheduling scheme significantly improves both the capacity to support deterministic service levels and resource utilization efficiency under mixed traffic flows with diverse requirements compared to a standard CG scheduling.

II. State of the Art

The 3GPP standard [4] defines two types of Configured Grant (CG). In *Type 1*, the uplink grant is configured through Radio Resource Control (RRC) signaling. In *Type 2*, RRC signaling only defines the grant's periodicity, while the uplink grant is signaled, activated, and deactivated using the PDCCH control channel, similar to Semi-Persistent Scheduling (SPS). CG Type 2 and SPS offer greater flexibility, enabling the dynamic adaptation of the configured grant based on changes in network or traffic conditions. Several studies have explored methods to enhance the adaptability of semi-static scheduling, improving its effectiveness while optimizing radio resource utilization. For example, [5] uses offline and online learning to dynamically adjust resource allocations in CG scheduling. The proposal continuously monitors parameters such as node buffer status and wasted resources to dynamically determine an optimal allocation strategy that minimizes the cumulative buffer status of UEs while ensuring a fair distribution of resources. The proposal reduces latency under stable traffic and channel conditions but faces challenges in highly dynamic environments. In [6], the authors propose a learning-based approach to periodically determine and adjust the allocation of radio resources for CG scheduling. The study

This work has been partially funded by the European Commission Horizon Europe SNS JU 6G-SHINE (GA 101095738) project, and by MCIN/AEI/10.13039/501100011033 (PID2023-150308OB-I00), and the "European Union NextGenerationEU/PRTR" (TED2021-130436B-I00), by Generalitat Valenciana and UMH's Vicerrectorado de Investigación grants.

focuses on using CG with shared resources for uplink traffic in a massive Machine-Type Communication (mMTC) scenario with heterogeneous MTC devices. The proposed scheme organizes nodes into priority-based groups based on their requirements and dynamically adjusts resource allocations according to the estimated traffic arrival rate and priority level. Similarly, [7] explores a scenario where mMTC and eMBB nodes share radio resources. mMTC nodes sense transmissions from eMBB nodes to detect patterns and use reinforcement learning to autonomously select radio resources in a grant-free scheduling framework, thereby avoiding collisions with eMBB transmissions. Despite the gains achieved, shared resources can compromise the ability to meet bounded latency deadlines for deterministic services, particularly as traffic demand increases.

Several studies propose leveraging predictive techniques to forecast traffic demand and proactively schedule resource allocations. For instance, [8] introduces a scheduling scheme that assigns radio resources within a scheduling window of m consecutive slots to the highest-priority nodes. A node's priority is determined based on factors such as the amount of buffered data, the predicted data generation in the next scheduling period of m slots, and the predictive average data rate for the upcoming m slots. In [9], the authors propose using proactive grants to allocate resources based on predictions of the data different nodes are expected to generate. A first approach predicts data sizes and allocates the necessary radio resources for each user in every slot. While this minimizes latency, it leads to over-reserving radio resources that may go unused. A second approach enhances efficiency by predicting both data sizes and traffic generation times. However, inaccuracies in traffic predictions can cause some packets to experience increased latency. In this context, this study progresses the state-of-the art with a novel predictive CG scheduling scheme that pre-allocates resources based on traffic predictions and prediction inaccuracies. By considering these inaccuracies, the scheme improves the ability to meet bounded latency requirements, and hence support deterministic services.

III. Predictive Configured Grant Scheduling

We consider a scenario with N nodes, where each node i (i=0, 1,…,N-1) generates data with an inter-packet generation time characterized by a mean value p_i and a standard deviation σ_i^t. The packet size is also characterized by a mean value s_i and a standard deviation σ_i^s. Each packet has a latency requirement L_i. Without loss of generality, we consider $p_i = p$ ms for all N nodes. The proposed predictive CG scheduler determines the radio resources to be allocated for all nodes within a scheduling interval of p ms, and scheduling decisions can be updated at every scheduling interval p. Resources are proactively pre-allocated to maximize the likelihood of satisfying the requirements of each transmission. To achieve this, a predictor forecasts the generation time $\hat{t}_i$ and size $\hat{s}_i$ of the next packet pkt_i for each node within the upcoming scheduling interval p. The scheduler then calculates the number of resources required for transmitting each packet pkt_i, considering not only the predicted size $\hat{s}_i$ but also a margin Δs_i to account for prediction inaccuracies; Δs_i can be set equal to the standard deviation σ_i^s or other value related to the prediction inaccuracy. We assume a NR radio interface where a radio resource is defined by a Resource Block (RB) in the frequency domain and a slot in the time domain. The scheduler estimates the number of RBs needed for pkt_i as $R_i = f(\hat{s}_i+\Delta s_i, mcs_i)$, where $f(\cdot)$ is a function that determines the number of RBs required to transmit a packet of size $\hat{s}_i+\Delta s_i$ using a Modulation and Coding Scheme (MCS) mcs_i following [4]. The proposed scheduler seeks to allocate R_i RBs for pkt_i within the allocation window $w_i=w(t_i^{ini}, t_i^{end})$, where $t_i^{ini} = \hat{t}_i+\Delta t_i$ and $t_i^{end} = \hat{t}_i-\Delta t_i+L_i$, $\hat{t}_i$ is the predicted generation time of pkt_i and Δt_i is a time margin to account for prediction inaccuracies of the generation time. The w_i ensures that a packet generated between $\hat{t}_i-\Delta t_i$ and $\hat{t}_i+\Delta t_i$ can be transmitted within its latency requirement L_i, as shown in Fig. 1. The scheduler identifies w_i for all packets pkt_i within the scheduling interval p, and searches for a scheduling solution that meets the latency requirements of the maximum possible number of packets. We assume a mixed traffic flow scenario where packets may have different latency requirements.

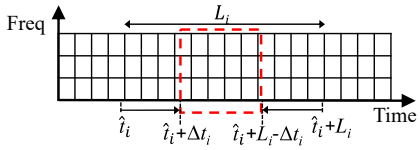

Fig. 1. Allocation window w_i for packet pkt_i.

The operation of the proposed predictive CG scheduling scheme is presented in Algorithm I. The scheme defines the set Φ, which is initialized with all the packets pkt_i scheduled for the next scheduling interval p. The scheduler starts processing packets with the shortest latency requirements (line 2 in Algorithm I). For each packet pkt_i, the scheduler first searches for available RBs within its allocation window w_i that do not overlap with the allocation window w_j of other packets pkt_j ($\forall j\neq i$) (line 3 of Algorithm I). We define this non-overlapping area of w_i as $w_i^{no} = w(t_i^{no\text{-}i}, t_i^{no\text{-}e})$. If the number of available RBs R_i^{no} within w_i^{no} is smaller than R_i ($R_i = f(\hat{s}_i+\Delta s_i, mcs_i)$), then pkt_i is added to an auxiliar set Θ as a pending packet awaiting RB allocation. Conversely, if $R_i^{no} \geq R_i$, the scheduler allocates R_i RBs to pkt_i within w_i^{no} (lines 4-9 of *Search_in_non-overlapping_area*). If multiple allocation options exist, the scheduler follows the policy outlined in *allocate_RB*. In particular, if w_i does not overlap with any other w_j ($\forall j\neq i$), the scheduler allocates RBs for pkt_i at the center of w_i. This increases robustness against inaccuracies in the estimated generation time of pkt_i. If w_i partially overlaps with the allocation window w_j of other packets, the scheduler prioritizes allocating resources from the boundary of w_i^{no} that is furthest from the respective limits t_i^{ini} or t_i^{end} of w_i. This ensures that packets generated with a deviation larger than Δt_i from the estimated time $\hat{t}_i$ can still meet their latency requirements. Once pkt_i receives RBs, it is removed from Φ (line 10 in *Search_in_non-overlapping_area*), and w_i is no longer considered when allocating RBs for other packets pkt_j ($j\neq i$). After completing the allocation process for all packets in Φ, the process in lines 2-13 in *Search_in_non-overlapping_area* is repeated for the remaining packets in Θ. We should note that a packet pkt_j that previously had $R_i^{no}<R_i$ might now have $R_i^{no}\geq R_i$ after removing from Φ the packets pkt_j that successfully received RBs. This iterative process continues until no further packets can be allocated the required R_i resources within non-overlapping areas.

For packets that cannot be assigned the required resources R_i within non-overlapping areas, the scheduler follows *Search_in_overlapping_area* (line 5 in Algorithm I). The process begins with packets that have the lowest latency requirements. For each packet pkt_i remaining in Φ after

Algorithm I: Predictive CG Scheduling
Input: set Φ of packets to schedule, $\hat{t}_i$, Δt_i, $\hat{s}_i$, Δs_i, L_i $\forall i$
1. Define for each pkt_i in Φ: $R_i = f(\hat{s}_i+\Delta s_i, mcs_i)$, $w_i=w(t_i^{ini}, t_i^{end})$, $t_i^{ini}= \hat{t}_i+ \Delta t_i$, $t_i^{end}= \hat{t}_i+ L_i - \Delta t_i$
2. Sort packets in Φ by L_i
3. Call Φ=*Search_in_non-overlapping_area*(Φ)
4. If $\Phi \neq \emptyset$ (there are packets without RBs)
5. Call *Search_in_overlapping_area*(Φ)
6. End procedure

Procedure I: *Search_in_non-overlapping_area*(Φ)
1. Set $\Theta = \emptyset$ (Θ is a set with pending packets)
2. Repeat
3. M = size(Φ)
4. For each pkt_i in Φ
5. Identify non-overlapping area $w_i^{no} = w(t_i^{no\text{-}i}, t_i^{no\text{-}e})$ between w_i and w_j $\forall j\neq i$ and pkt_j in Φ
6. R_i^{no} = available RBs within w_i^{no}
7. If $R_i^{no} \geq R_i$
8. Allocate R_i RBs in w_i^{no} to pkt_i: call *allocate_RB*
9. Else $\rightarrow$ pkt_i is included in Θ
10. Removed pkt_i from Φ
11. End For
12. $\Phi = \Theta$, $\Theta = \emptyset$
13. Until size(Φ) == M
14. Return Φ and end procedure

Procedure II: *allocate_RB*(pkt_i, w_i^{no}=$w(t_i^{no\text{-}i},t_i^{no\text{-}e})$, R_i, t_i^{ini},t_i^{end})
1. If $t_i^{no\text{-}i}$== t_i^{ini} & $t_i^{no\text{-}e}$== t_i^{end}
2. Allocate R_i RBs in the center of w_i^{no}
3. Elseif $t_i^{no\text{-}i}$-t_i^{ini} > t_i^{end} - $t_i^{no\text{-}e}$
4. Allocate R_i RBs in w_i^{no} starting from $t_i^{no\text{-}i}$
5. Else
6. Allocate R_i RBs in w_i^{no} ending at $t_i^{no\text{-}e}$
7. End procedure

Procedure III: *Search_in_overlapping_area*(Φ)
1. For each pkt_i in Φ
2. Repeat
3. R = available RBs within w_i= $w(t_i^{ini}, t_i^{end})$
4. If $R \geq R_i$ $\rightarrow$ Allocate R_i RBs in w_i to pkt_i
5. Elseif odd iteration $\rightarrow$ t_i^{end}=t_i^{end}+Δt_i
6. If even iteration $\rightarrow$ t_i^{ini}= t_i^{ini}-Δt_i
7. Until pkt_i receives RBs or w_i==$w(\hat{t}_i$-Δt_i, $\hat{t}_i$+L_i+$\Delta t_i)$
8. If pkt_i has not received RBs & $R_i > f(\hat{s}_i, mcs_i)$
9. $R_i = f(\hat{s}_i, mcs_i)$, $t_i^{ini}= \hat{t}_i+ \Delta t_i$, $t_i^{end}= \hat{t}_i+ L_i - \Delta t_i$
10. Goto line 2
11. End For
12. End procedure

Search_in_non-overlapping_area, the scheduler checks whether there are sufficient RBs within w_i to satisfy R_i ($R_i = f(\hat{s}_i+\Delta s_i, mcs_i)$). If so, the scheduler allocates R_i RBs within w_i to pkt_i (lines 3-4 in *Search_in_overlapping_area*). If there are insufficient RBs, the size of w_i is iteratively augmented by Δt_i until there are sufficient RBs available within w_i to satisfy R_i, or w_i reaches its maximum possible size L_i+2·Δt_i (lines 5-7 in *Search_in_overlapping_area*). The maximum size is defined so that it is still possible to meet the latency requirement L_i if the packet is generated at $\hat{t}_i$+Δt_i or $\hat{t}_i$-Δt_i. If w_i reaches its maximum allowed size, the scheduler reduces the number of RBs to allocate for pkt_i to match only the predicted size (i.e., R_i is updated as $R_i = f(\hat{s}_i, mcs_i)$), and searches again for R_i RBs in w_i for pkt_i (lines 8-10 in *Search_in_overlapping_area*). Increasing w_i reduces the likelihood of meeting the latency requirement for packets that deviate significantly from their expected generation time $\hat{t}_i$, but the requirement can still be satisfied in some cases. For example, consider the case where t_i^{end} is equal to t_i^{end}= $\hat{t}_i$+L_i, and the scheduler finds RBs for pkt_i at the end of w_i as illustrated in Fig. 2. In this case, the latency requirement L_i cannot be met if pkt_i is actually generated before $\hat{t}_i$ as

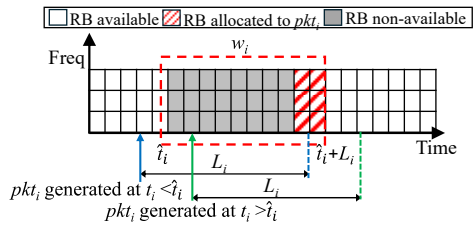

Fig. 2. Example of packet pkt_i generated at t_i for which its latency requirement L_i is satisfied when $t_i < \hat{t}_i$ but not when $t_i < \hat{t}_i$.

illustrated in Fig. 2, but it can still be satisfied if pkt_i is generated after $\hat{t}_i$.

IV. Traffic Characterization and Prediction

The proposed predictive CG scheduler pre-allocates resources for future traffic demands by leveraging predicted traffic information while accounting for potential prediction inaccuracies. To evaluate our proposal, we consider a 6G-envisioned autonomous driving scenario in which sensor data generated by an autonomous vehicle is sent to the network for processing at the edge [10]. Communications must meet a bounded latency deadline to ensure that offloading processing workloads to the network does not disrupt vehicle operations. For our evaluation, we use realistic sensor data generated by autonomous vehicles through a Connected and Automated Mobility (CAM) platform [11]. This platform integrates realistic sensing and autonomous driving (AD) capabilities using the open-source CARLA and AUTOWARE software. We have configured the autonomous vehicle in the CAM platform with a full suite of Level 3 (L3) AD sensors, including five cameras and five radars mounted on the top, front, rear and sides of the vehicle. Each sensor is considered a data source or node in our evaluation, requiring offloading of its traffic to the network. The offloaded traffic includes detected objects such as vehicles, obstacles and pedestrians. Sensors generate raw data at periodic intervals, which is then processed by a perception module to extract detected objects. We have collected extensive datasets of processed sensor packets including their size and timestamp from realistic urban environments (Fig. 3).

The different sensors have a sampling rate of 20 Hz, collecting data every 50 ms. Then, the object detection algorithm introduces a processing delay that depends on the driving scenario and the number of detected objects. We have characterized this processing delay for each sensor, showing a standard deviation ranging from 1.47 to 1.80 ms. Following the nomenclature used in Section III, the proposed predictive CG scheme considers 50 ms as the inter-packet generation time p, $\hat{t}_i$ is estimated as t_i^0+p where t_i^0 is the generation time of the first packet for each sensor i of the N=10 sensors, and Δt_i is set to the characterized standard deviation value σ_i^t.

The size of processed sensor packets varies significantly, as shown in Fig. 3, since it depends on the number of objects

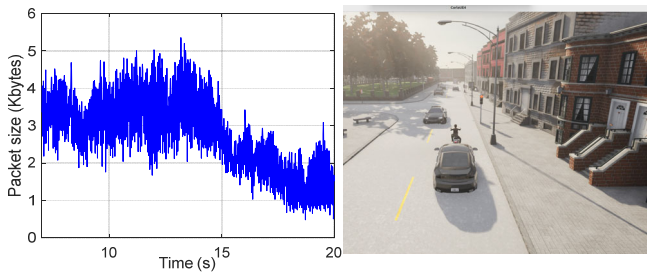

Fig. 3. Sample trace of processed sensor data packets.

detected in the driving scenario. To predict the size of future processed sensor packets, we implemented a predictor based on a Long Short-Term Memory (LSTM) network using regression-based supervised learning. LSTM networks are particularly suited for tasks involving sequential or time-series data, where the order and context of input elements are relevant. This includes tasks where dependencies between data points over time need to be learned, making it suitable for predicting autonomous vehicle sensor data since the size of each packet is tied to past packets and sensor behaviors. The hyper-parameters used for the configuration of the LSTM are summarized in Table I and were optimized to minimize the Mean Absolute Error (MAE), which quantifies the average magnitude of prediction errors as MAE=$\sum_{i=1}^{P}|s_i-\hat{s}_i|/P$, where P represents the number of predicted packets, s_i is the actual packet size, and $\hat{s}_i$ is the predicted packet size. We used a dataset containing 9780 samples, with 60% allocated for training the LSTM, 20% for validation, and the remaining 20% for testing. The LSTM network is configured to predict the size of the next ten packets, i.e. the processed sensor packets generated by each of the N=10 sensors within the period p=50 ms. Fig. 4 shows the CDF (cumulative distribution function) of the absolute error for the prediction of the first, fifth and tenth packets. The figure illustrates the magnitude of possible prediction inaccuracies and reinforces the need to account for such inaccuracies when reserving resources based on predicted traffic demands. As described in Section III, the proposed predicted CG scheduling scheme accounts for the inaccuracy of the predicted packet size $\hat{s}_i$ when determining the resources that should be pre-allocated to each pkt_i to minimize the impact of prediction errors on the capacity to meet the latency requirements.

TABLE I. LSTM HYPER-PARAMETERS

Parameter	Value	Parameter	Value
Sequence Length	150	Number of layers	3 (units: 256,128,64)
Batch Size	32	Features Per Sample	6
Dropout	0.1	Epochs	100
Optimizer	Adam	Scaling Method	Min-Max Scaling
Learning rate	0.001	Number of Outputs	10

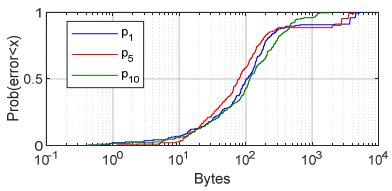

Fig. 4. CDF of the absolute prediction error ($|s_i - \hat{s}_i|$).

V. EVALUATION AND DISCUSSION

This section compares the performance of the proposed predictive CG scheduler (PCG) against a reference (non-predictive) 5G CG scheduling scheme. The reference scheme periodically allocates RBs for transmitting packets generated by each node. Following [12], the reference scheme allocates RBs to minimize the latency of each packet. For a fair comparison with PCG, the reference scheme uses an allocation period p=50 ms and seeks to allocate RBs to pkt_i within w_i = w(t_i^{ini}, t_i^{end}) with $t_i^{ini}=\hat{t}_i+\Delta t_i$, $t_i^{end}=\hat{t}_i-\Delta t_i+L_i$, and $\Delta t_i=\sigma_i^t$, which ensures that a packet generated between $\hat{t}_i-\Delta t_i$ and $\hat{t}_i+\Delta t_i$ can be transmitted within its latency requirement L_i. The reference scheme allocates the amount of RBs necessary to transmit packets of size S_i. We test different configurations of the reference scheme where S_i is established based on the most frequent value of the packet sizes, i.e., the mode of the packet size -mode(s_i)- (C1 configuration), or on the 80th, 90th, 95th, and 99th percentiles of the packet size (C2, C3, C4 and C5 configurations for the reference scheme), respectively. The percentile value is represented by the function $P_x(s_i)$, where x represents the desired percentile. We also evaluate different configurations of the proposed PCG scheduler to assess the impact of the selection of the prediction inaccuracy Δs_i. PCG is evaluated with values of Δs_i equal to the standard deviation of the predicted size σ_i^s (C1 configuration for PCG), or equal to the 80th, 90th, 95th, or 99th percentiles of the absolute error of the prediction, i.e., $P_x(AE)$ with x=80, 90, 95 and 99, and $AE=|s_i-\hat{s}_i|$ (C2, C3, C4 and C5 configurations for PCG, respectively). Table II shows the evaluated configurations for PCG and the reference schemes. In addition, we also evaluate a predictive CG scheduler that allocates RBs for packet transmissions following a scheduling policy similar to PCG but only considering the predicted packet size $\hat{s}_i$ and not taking into account prediction inaccuracies.

TABLE II. EVALUATED CONFIGURATIONS FOR PCG AND REF.

Scheduler	Configurations				
	C1	C2	C3	C4	C5
PCG	$\Delta s_i = \sigma_i^s$	$\Delta s_i=P_{80}(AE)$	$\Delta s_i=P_{90}(AE)$	$\Delta s_i=P_{95}(AE)$	$\Delta s_i=P_{99}(AE)$
Reference	S_i=mode(s_i)	$S_i=P_{80}(s_i)$	$S_i=P_{90}(s_i)$	$S_i=P_{95}(s_i)$	$S_i=P_{99}(s_i)$

The performance of the proposed PCG scheme and the reference scheme is evaluated considering a 5 MHz cell bandwidth, a 30 kHz NR subcarrier spacing (SCS) [4] and a MCS11 (Modulation and Coding Scheme) to balance between robustness and spectral efficiency; similar trends have been observed for other configurations. We consider a mixed traffic flow scenario with latency requirements derived from 3GPP specifications for enhanced V2X scenarios [13]. We consider that 50%, 25% and 25% of the packets must be transmitted within a maximum latency of 50, 20 and 10 ms, respectively; other scenarios with mixed traffic flows and different latency requirements have also been evaluated, and similar trends have been observed.

Fig. 5 presents the percentage of transmissions that meet their latency requirements using the proposed PCG scheme and the reference (Ref.) scheme. The performance is shown for the different configurations evaluated for each scheme following Table II. Fig. 5 shows that PCG significantly increases the percentage of packets that meet their latency requirements compared to the reference scheme. PCG can reach satisfaction levels higher than 87% with all the evaluated configurations, while the reference scheme cannot surpass a 64% satisfaction level regardless of the configuration used. Fig. 5 also reports the performance achieved with a predictive configured grant scheme that does not consider prediction inaccuracies and pre-allocates resources based only on the predicted packet size $\hat{s}_i$. In this case, only about 64% of packets meet their latency requirement (similar to the reference scheme) compared with a satisfaction level of 92.4% and 98.9% with the PCG when $\Delta s_i=\sigma_i^s$ (C1) and $\Delta s_i=P_{99}(AE)$ (C5) respectively. These results strongly highlight the importance of accounting for prediction inaccuracies in the design of predictive scheduling schemes capable of supporting deterministic communications[1].

[1] We should note that the transmissions that PCG cannot satisfy correspond to packets with a size larger than $\hat{s}_i + \Delta s_i$. In this case, the number of allocated RBs is insufficient for transmitting these packets in time to meet their latency requirement.

Fig. 5 shows that the proposed PCG increases its performance as the prediction inaccuracy Δs_i is set equal to higher percentile values of the prediction's absolute error. Similarly, the reference scheme increases its satisfaction level when it allocates RBs based on the highest percentiles of the packet size. However, these improvements come at the expense of pre-allocating a larger number of RBs per packet than actually needed, thus reducing resource efficiency. This is illustrated in Fig. 6, where Fig. 6.a represents the percentage of RBs allocated for the transmission of packets and Fig. 6.b represents the percentage of pre-allocated RBs that are actually unutilized. Fig. 6.a shows that the percentage of allocated RBs increases for PCG when Δs_i is set equal to higher percentile values of the prediction's absolute error, and increases for the reference scheme when allocating RBs based on the highest size percentiles. However, PCG pre-allocates in general a lowest number of RBs than the reference scheme while achieving higher satisfaction levels (Fig. 5). In addition, PCG results in a significantly lower percentage of non-utilized RBs compared to the reference scheme, which highlights its highest resource efficiency.

Following the URLLC principles in 5G, the reference scheme focuses on minimizing the transmission latency. On the other hand, PCG has been designed to support deterministic communications in beyond 5G networks, and hence prioritizes maximizing the number of transmissions that meet their latency requirements. Fig. 7 plots the cumulative distribution function (CDF) of the latency experienced by packets with 10, 20, and 50 ms latency requirements, respectively. The figure shows that packets with the most stringent latency requirement (10 ms) experience the lowest latency values when using the PCG scheme. On the other hand, PCG slightly increases the latency of packets with more relaxed latency constraints. This is particularly the case for packets with a 20 ms requirement as these packets often compete for the same RBs as the packets that require 10 ms latency. PCG intentionally delays the transmission of packets with more relaxed latency requirements, while still meeting their latency deadline, to ensure that packets with tighter deadlines can be transmitted in time. In contrast, a scheduler that seeks minimizing the transmission latency (Ref.) does not leverage varying latency requirements in mixed traffic flows to increase the percentage of satisfied transmissions, and the latency experienced increases uniformly up to the maximum allowed latency.

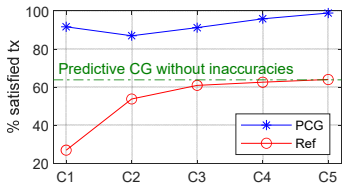

Fig. 5. Percentage (%) of transmissions meeting their latency requirements.

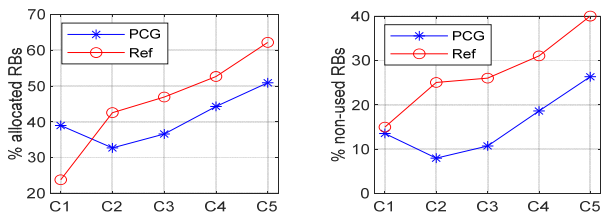

a) Allocated RBs. b) Allocated but non-used RBs.

Fig. 6. Percentage of allocated RBs and percentage of allocated RBs that are non-used for packet transmissions.

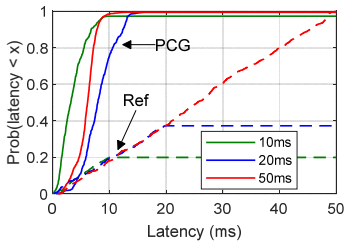

Fig. 7. CDF of the latency experienced by packets with 10, 20 and 50 ms latency requirements with PCG and the reference scheme.

VI. Conclusions

This study presents a novel predictive configured grant scheduling scheme designed to support deterministic communications in beyond 5G networks. The proposed predictive CG scheduling scheme pre-allocates resources based on traffic predictions and prediction inaccuracies with the objective to maximize the percentage of packets transmitted within their bounded latency requirements. The evaluation shows that the proposed predictive CG scheme significantly increases the percentage of satisfied transmissions compared to a 5G CG scheduler while pre-allocating less resources and using them more efficiently. Our evaluation has also demonstrated the importance of accounting for prediction inaccuracies in the scheduling process to improve the ability to meet bounded latency requirements and hence support deterministic services in beyond 5G networks.

References

[1] Yungang Pan, et al., "Resource Optimization with 5G Configured Grant Scheduling for Real-Time Applications", in *Proc. Design, Automation & Test in Europe Conference & Exhibition (DATE)*, Antwerp, Belgium, 2023, pp. 1-2.

[2] A. Larrañaga-Zumeta, M.C. Lucas-Estañ, J.Gozálvez, A. Arriola, "5G configured grant scheduling for seamless integration with TSN industrial networks", *Computer Communications*, vol. 226–227, 107930, 2024.

[3] A. Valcarce, et al., "The Role of AI in 6G MAC", in *Proc. 2024 Joint European Conference on Networks and Communications & 6G Summit (EuCNC/6G Summit)*, Antwerp, Belgium, 2024, pp. 723-728.

[4] 3GPP, TS 38.300. V17.11.0, "NR; NR and NG-RAN Overall Description; Stage 2 (Release 18))", Release 17, 2024.

[5] M. Elsayem, et al., "Intelligent Resource Allocation for Grant-Free Access: A Reinforcement Learning Approach", *IEEE Networking Letters*, vol. 5, no. 3, pp. 154-158, Sept. 2023.

[6] Y. Kaura, et al., "Adaptive Scheduling of Shared Grant-Free Resources for Heterogeneous Massive Machine type Communication in 5G and Beyond Networks", *IEEE Transactions on Network and Service Management*, Early Access, Nov. 2024.

[7] G. Di Gennaro, et al., "Decentralized Grant-Free mMTC Traffic Multiplexing With eMBB Data Through Deep Reinforcement Learning", *IEEE Transactions on Machine Learning in Communications and Networking*, vol. 2, pp. 1440-1455, Sept. 2024.

[8] Q. He, G. Dán and G. P. Koudouridis, "Semi-Persistent Scheduling for 5G Downlink based on Short-Term Traffic Prediction", in *Proc. of the IEEE Global Communications Conference* (GLOBECOM 2020), Taipei, Taiwan, 2020, pp. 1-6.

[9] D. Overbeck, et al., "Proactive Resource Management for Predictive 5G Uplink Slicing", in *Proc. of the 2022 IEEE Global Comms. Conf.* (GLOBECOM 2022), Rio de Janeiro, Brazil, 2022, pp. 1000-1005.

[10] 6G IA, *European Vision for the 6G Network Ecosystem*, v2, 2024.

[11] L. Lusvarghi, et al., "Characterization of In-Vehicle Network Sensor Data Traffic in Autonomous Vehicles", in *Proc. 2024 IEEE Vehicular Networking Conference (VNC)*, Kobe, Japan, May, 2024.

[12] A. Omer, et al., "Performance Evaluation of 5G Delay-Sensitive Single-Carrier Multi-User Downlink Scheduling", in *Proc. IEEE 34th Annual International Symposium on Personal, Indoor and Mobile Radio Communications* (PIMRC), Toronto, Canada, 2023, pp. 1-6.

[13] 3GPP, TS 22.186. V17.0.0, "Enhancement of 3GPP support for V2X scenarios", Release 17, 2022.